

# Creep Behavior of Basalt and Glass Fiber Reinforced Epoxy Composites

Reza Eslami Farsani<sup>1</sup>, Seyed Mohammad Reza Khalili<sup>2\*</sup>, Vahid Daghighi<sup>3</sup>, Reza Fazaeli<sup>4</sup>

Received: 9 May 2011; Accepted: 26 Nov. 2011

**Abstract:** Basalt fibers enjoy the best potential to be turned into a serious contender in fiber composite market due to its good mechanical properties and favorable costs. The creep behavior of basalt fiber reinforced epoxy (BFRE) and glass fiber reinforced epoxy (GFRE) composites was studied through tensile testing at a high temperature. To study the effect of reinforcing epoxy, the micro glass powder (MGP) was added at various volume percentage into the epoxy resin in BFRE composites. The initial strain for all the specimens were evaluated and compared with each other. No creep rupture failures were observed in short-term (less than 10000 seconds) high temperature ( $T= 150$  and  $200$  °C) tensile creep tests at the loads up to 15% of the ultimate tensile strength of the specimen. It was also found that the creep resistance of BFRE was higher than that of GFRE and the materials are generally behaved as non-linear for all stresses and temperatures. Adding MGP decreased the initial strain of BFRE, but had no significant effect on the overall life time of BFRE.

**Keywords:** Creep Analysis, Basalt Fiber Reinforced Composites, Glass Fiber Reinforced Composites

## 1. Introduction

Nowadays, polymer composite materials are going to be substituted for traditional materials in many industrial applications due to their excellent strength to weight ratio, high fatigue and corrosion resistance, favorable price and ease of fabrication and shape [1]. Therefore, there is always a great need for further experiments to have a comprehensive knowledge about these materials. Nevertheless, there is rarely research on creep properties of the ilk of materials. Kawai and Sagawa [2] studied the stress-time-temperature extrapolation of off-axis creep rupture on a T800H/2500 unidirectional carbon/epoxy laminate. Off-axis tensile creep rupture tests were performed on plain coupon specimens with five kinds of fiber orientations  $\Theta = 0, 10, 30, 45$  and  $90$  ° at each of the test temperatures of 60, 80 and 130 °C, respectively, within the time range of up to 10 h. They used either a formula derived from a modified damage mechanics model or a formula on the basis of a grand master creep rupture curve built by means of a non-dimensional effective stress and the

Larson-Miller parameter. Dasappa et al. [3] studied the effects of temperatures on the tensile creep continuous random fiber glass mat thermoplastic composite (GMT), following an accelerated characterization procedure. They tried to obtain a long-term creep model using time-temperature superposition that could represent behavior within the linear viscoelastic regime (up to 20 MPa) at room temperature. They also aimed to develop a non-linear viscoelastic model that accounts for a wide range of stress between 20 and 60 MPa over a temperature range of room temperature to 90 °C. It was found that the material generally behaved non-linearly for all stresses. Their model predictions were in good agreement with the experimental results at most stress and temperature levels. They showed that creep curves could predict at higher temperatures especially at 60 MPa tend to underestimate at a longer time.

Kouadri-Boudjelthia *et al.* [4] studied the effects of temperature on creep parameters of composite material made of unsaturated polyester and reinforced with randomly oriented type C glass fibers. They carried out the experimental study to determine evolution of the law

1. Assistant Professor, Faculty of Mechanical Engineering, K. N. Toosi University of Technology, Tehran, Iran (eslami@kntu.ac.ir)

2\*. Corresponding Author: Faculty of Mechanical Engineering, K. N. Toosi University of Technology, Tehran, Iran (khalili@kntu.ac.ir)

3. M. Sc., South Tehran Branch, Islamic Azad University, Tehran, Iran (vahid.daghighi\_del@yahoo.com)

4. Assistant Professor, South Tehran Branch, Islamic Azad University, Tehran, Iran (r\_fazaeli@azad.ac.ir)

in the function of relevant parameters. The experiments were then used to identify the phenomenological relationship and its appointed coefficients. Guedes et al. [5] studied the influence of moisture absorption on longterm creep behavior of glass-reinforced thermo-setting plastic (GRP) pipes. These pipes were used in water transportation which had an effect on the mechanical properties and on the polymeric composite matrix. Ten specimens were tested as delivered. Another 10 specimens were conditioned in water at room temperature and another 10 were conditioned in water at 50 °C, until saturation. They applied the time-temperature superposition principle (TTSP) and extrapolation using a power law relation to dynamic mechanical thermal analysis (DMTA) data for a long-term creep prediction. Both methods were found to be conservative, i.e. predicted higher stiffness reduction than the creep tests. Although creep tests were quite dissimilar from the DMTA tests, extrapolation using a power law relation appeared to be accurate enough to be used as a predictive tool for project design. Goertzen and Kessler [6] studied the creep behavior of a carbon fiber/epoxy matrix composite through tensile and flexural creep testing. For elevated temperature, flexural creep compliance data taken at isotherms between 30 and 75 °C, the principal of time-temperature superposition held. They showed that the constant activation energy assumption worked fairly well, but only for temperatures below the onset of T<sub>g</sub> of the material.

Whilst epoxy resins, one of the most prevalent resins utilized in manufacturing polymer matrix composites, are usually highly cross-linked polymers with a glass transition temperature above ambient temperature, they still demonstrated visco-elastic behavior [7]. Consequently, the properties may change with time under the load. Under long-term loading, mechanical properties will encounter an ongoing decline with time and stress and strain levels in the composite specimens will vary considerably from measurements computed using property data attained from short term tests [8]. With increasing time under load, the stiffness of the material not only decreases with time, but the decrease rate ascends with stress giving rise to an indicative complex behavior. In order to reduce the rate at which the stiffness of the composite alters and to perpetuate the stiffness of the composite to a definite degree to tolerate long duration loading and environmental conditions, the resin of the composite can be reinforced through either chemical methods analysis and polymer structure change of the resin or adding different filler such as alumina or silica [9].

Glass fibers are widely used in composite; industry; however, on the other hand, during recent years few researchers have paid attention to high potential of basalt fibers thanks to suitable price, its appropriate mechanical performance as well as its capability for replacing in resin reinforced fiber composites with comparable glass fibers [10-12]. Wei et al. [11] studied bolstering up basalt fiber roving with nano-SiO<sub>2</sub>-epoxy composite coating. They showed that the SiO<sub>2</sub> nano particle-epoxy composite coating could increase the tensile strength of the basalt fibers in comparison with the pure epoxy coating. Besides, coating could provide the basalt fibers an auspicious interfacial property in the basalt fiber reinforced composites. Lopresto et al. [12] carried out some mechanical tests on comparable E-glass and basalt fiber reinforced plastic laminates to evaluate the feasibility of substituting basalt fibers for glass fiber composites. The results attained on the two laminates were juxtaposed illustrating excellent function of basalt fibers in terms of impact force and energy, Young's modulus, compressive and bending strength. These promising properties can advocate achievable applications of basalt fibers in areas where glass fiber composites are mostly employed.

Colombo et al. [13] investigated basalt fibers composites through several static and fatigue tests. They compared the results with other composite materials in glass and carbon fibers. Wei et al. [14-15] studied environmental resistance and mechanical performance of treated basalt and glass fibers with sodium hydroxide hydrochloric acid solutions in various times. They expressed the mass loss ratio of the fibers and the strength maintenance ratios of the fibers. The acid resistance was better than the alkali resistance for the basalt fibers. Notwithstanding, for the glass fibers the situation was different: the acid resistance was nearly the same as the alkali resistance. Carmisciano et al. [16] performed a comparative investigation on basalt and E-glass woven fabric reinforced composites through flexural and interlaminar characterization. Woven patterns, the laminates and fiber volume fraction used for specimens were the same. They showed that basalt fiber composites had higher flexural modulus and interlaminar shear strength in comparison with E-glass ones, however a lower flexural strength and similar electrical properties.

Wei *et al.* [17] investigated degradation of basalt fiber and glass fiber/epoxy resin composites in seawater. The tensile and bending strength of seawater treated specimens showed a decreasing inclination with treatment time. It was found that the anti-seawater

corrosion property of the basalt fiber reinforced composites was approximately the same as that of glass fiber reinforced ones. Possible corrosion mechanisms indicated that an efficacious lowering of the  $Fe^{2+}$  content in the fiber could eventuate in better stability for the basalt fiber composites in seawater. Fiore *et al.* [18] studied glass-basalt/epoxy composites for marine applications. They used three point bending and tensile tests to evaluate the impact of number and position of basalt layers on the mechanical properties of composite structures. The output data showed that the existence of external layers of basalt can cause the highest escalation in mechanical properties of hybrid laminates compared to those of glass fiber reinforced plastics laminates.

This study for the first time is based on the experimental investigation of creep behavior of BFRE and comparing it to GFRE. To study the effect of adding micro glass particles, the micro glass particles in various volume fractions are added to BFRE and then compared to plain BFRE in creep loads.

## 2. Experimental procedures

### 2.1. Materials

Unidirectional Basalt fiber (Hengdian Group Shanghai Russia & Gold Basalt Fiber Co., china was provided with the following properties: thickness = 0.17 mm, surface density = 300 g/m<sup>2</sup>, density = 2.7 g/cm<sup>3</sup>. Unidirectional E-Glass fiber (Metyx Multiaxial Technology, Turkey) was provided with the following properties: surface density = 300 g/m<sup>2</sup>, density = 2.5 g/cm<sup>3</sup>. For fabrication of composites, the used epoxy resin was ML-506 with the Hardener HA-11 (Mokarrar Engineering Materials Co., Iran) which are produced on the basis of epoxy Bisphenol F and Polyamine Hardener with the following physical properties: density = 1.1 g/cm<sup>3</sup>, viscosity = 1450 centipoise. Mechanical properties of the resin are shown in Table 1.

The micro glass powder was provided through automatic sieving by means of mesh number ASTM 270, it means that all of the glass particles have a dimension equal to 53-62  $\mu$ m. The GFRE and BFRE samples were made by four layers through hand lay-up method and the layer sequencing was [0°]<sub>4</sub>. The BFRE lay-up was considered to study the effect of MGP in the resin. BFRE added by 2.5%, 5.5% and 8.5% volume fraction of MGP were prepared for this reason. The

powders were well dispersed by automatic mixer into the resin before combinations with basalt fibers. The fiber volume fractions for all samples are 25%.

### 2.2. Specimen preparation and fabrication

GFRE and BFRE pieces with the dimensions of 25 cm×30 cm were fabricated through hand lay-up method. The types and their corresponding specimen codes are shown in Table 2.

Application of gentle pressure (approximately 1.8 kPa) squeezed out the extra matrix for both GFRE and BFRE specimens. The specimens were then allowed to cure at room temperature (25 °C) and humidity 65%, for 8 days and were cut to dimensions required for creep test by means of abrasive water jet machine. The thickness of the specimens is 1.8 mm. Fig. 1 shows the schematic diagram of the specimens.

### 2.3. Creep test

Creep tests in the present work were conducted in accordance with ASTM D2990. The testing machine was a Torsee Creep and Rupture Testing machine (Fig. 2). The schematic diagram of the testing machine is shown in Fig. 3. The testing machine has three main unite, 1- loading mechanism, 2- heating system and 3-strain measuring system. The loading mechanism uses variable mass units to load the specimens. According to ASTM D2990, the loading operation should be continuous without any shock or interruption. The heating system has three heating units with variable heating power which enable the specimens to reach the testing temperature gradually without heat shock. Any displacement in the specimen was recorded using a gage with an accuracy of 0.005 mm. The specimens were fixed in the loading apparatus by means of a specific fixture (Fig. 4).

The temperatures considered for conducting creep tests were 150 °C and 200 °C. The specimens were inserted inside the grips and placed in the creep chamber. The system was given 25 min. to reach the specified temperature before loading. The temperature was checked using two digital temperature controllers during testing. The loading system in the testing machine enables the user to load the system gradually without any mechanical shock. The load applied to the specimens was 15% ultimate strength of each specimen.

### 3. Results and discussions

The results as a function of specimen codes and temperature are shown in Fig. 5 and 6. A time dependent function called creep compliance,  $D(t)$ , is used in the figs. This function is used in creep modeling of polymers and plastics [8] and is defined in Eq. (1), where  $\epsilon(t)$  is the instantaneous strain and is the constant stress applied to the specimens.

$$D(t) = \frac{\epsilon(t)}{\sigma_0} \quad (1)$$

**Table 1. Mechanical properties of the resin**

Item	Quantity	Unit	Standard
Compressive strength	974	kgf/cm <sup>2</sup>	ASTM D695M
Bending strength	960	kgf/cm <sup>2</sup>	ASTM D790M
Ultimate tensile strength	761	kgf/cm <sup>2</sup>	ASTM D638M
Hardness	82	Shore D	ASTM D2240
Toughness	7.85	KJ/ m <sup>2</sup>	ASTM D256

**Table 2. Codes of the specimens**

Code	Type	Code	Type
1	(a) GFRE+0% MGP	2	(b) BFRE+0% MGP
3	(c) BFRE+%2.5 MGP	4	(d) BFRE+%5.5 MGP
5	(e) BFRE+%8.5 MGP		

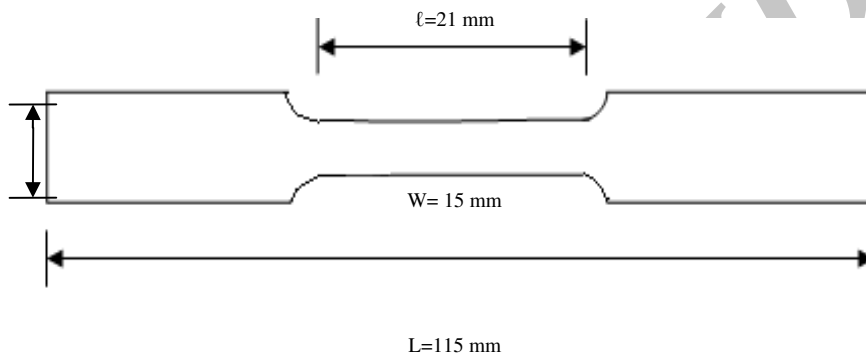


**Fig. 1. The schematic diagram of the specimens.**



**Fig. 2. Creep testing machine.**

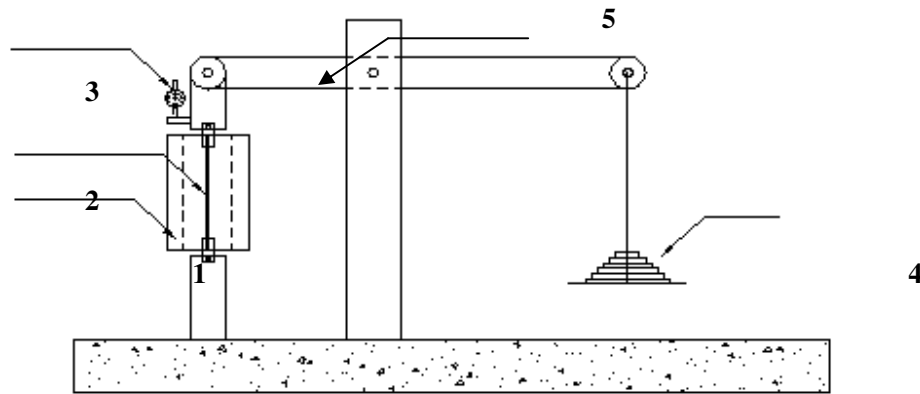


Fig. 3. Schematic diagram of the testing. 1- Isothermic enclosure, 2- Specimen, 3- Comparator, 4- Masses, 5- Arm of the lever.

Table 3. Creep information for various BFRE and GFRE

Specimen Code	T=150 °C					T=200 °C				
	1	2	3	4	5	1	2	3	4	5
Initial Strain after one minute ( $\times 10^{-2}$ )	10.91	21.49	20.82	19.6	17.87	9.8	20.13	19.72	18.63	17.15
Strain rate (1/s) during the first minute ( $\times 10^{-3}$ )	1.8	3.58	3.47	3.27	2.98	1.63	3.35	3.29	3.104	2.86

Fig. 5 shows the results obtained from the creep test for the specimen codes 1 to 5 at T=150 °C. The Fig. shows the creep compliance versus time and instantaneous strain and 0 fibers are along loading direction. The compliance and the strain are directly proportional to each other (Eq. (1)), and therefore, as shown in Fig. 5, the initial strain for all the specimens contained MGP has decreased. A series of tests were then performed to investigate the effect of changing temperature. The second selected temperature was 200 °C. Fig. 6 shows the results. Table 3 also illustrates the results in terms of initial strain and strain rate obtained from creep tests for various specimen codes at different temperatures and compared to each other. Figs. 5 and 6 show excellent creep properties of BFRE in comparison with GFRE. Prior to this, Khalili et al. had shown the superior performance of BFRE under bending and tensile loads compared to those of GFRE [10]. Fig. 7 shows GFRE specimen after creep test.

As it can be seen from Figs. 5 and 6 and Table 3, the initial creep strain or compliance have considerably decreased for all the specimen codes 3 to 5 which could be a sign of higher stiffness due to the presence of MGP, tending to maintain the specimen strain at a lower level. This could be an excellent method for designing pieces where large amounts of strain are not allowed. But the predicted failure time does not make any difference between the specimens with MGP and without MGP. The reason behind is that the effect of MGP is on the matrix not fiber and the fiber is ruling phase in creep test. Specifically, the matrix approaches to be ruined after some days. Though initial strain and initial strain rate during the first minute of the test performance for GFRE are less than those of BFRE at T=150 °C and 200 °C, it is clearly observed from Figs. 5 and 6 that the slope of the GFRE compliance is much more than that of BFRE during the whole test and therefore, creep resistance of BFRE is superior to that of GFRE.

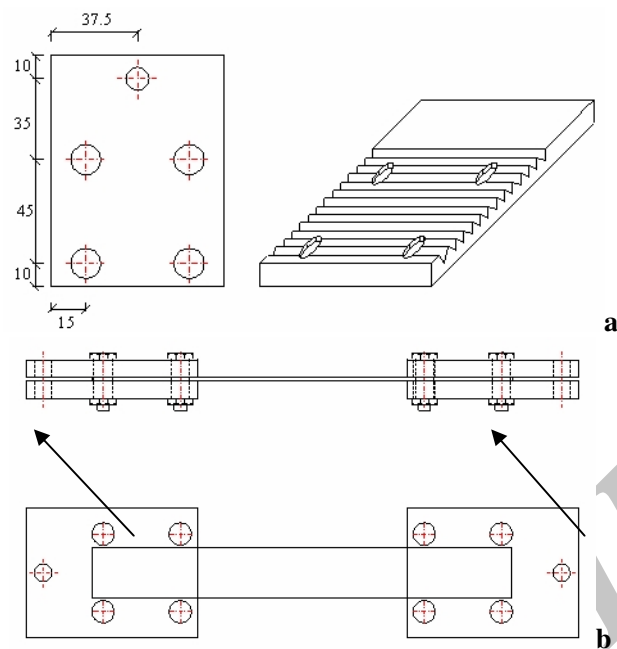


Fig. 4. Apparatus in creep testing machine, a. Fixture for holding the specimen, b. Hole for application of the load, specimen in the fixture.

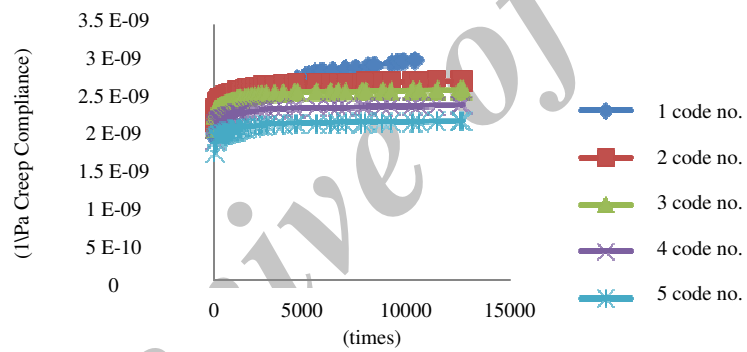


Fig. 5. Comparison between creep properties of BFREs and GFRE under 15% their ultimate strengths load at T=150 °C.

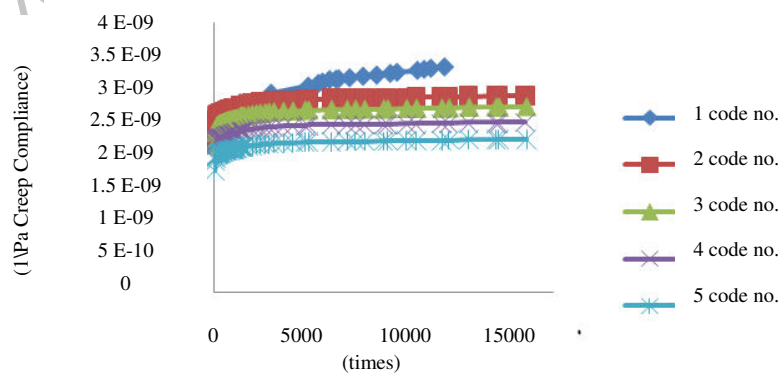


Fig. 6. Comparison between creep properties of BFRE and GFRE under 15% their ultimate strengths load at T=200 °C.

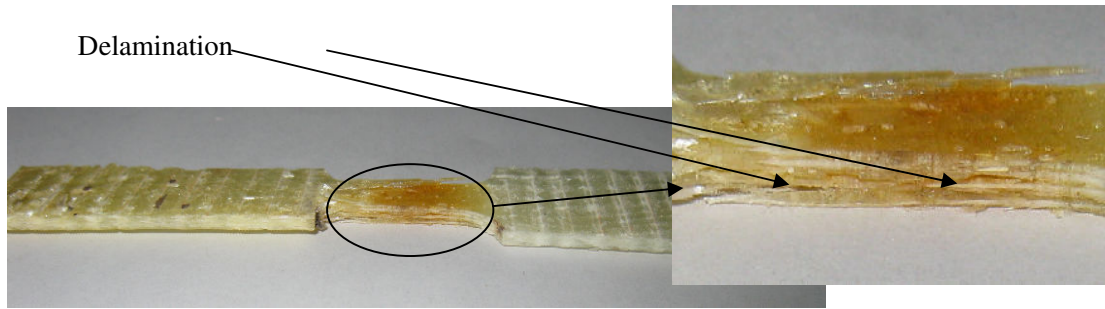


Fig. 7. GFRE specimen after creep test under 15% ultimate strength load at  $T=200\text{ }^{\circ}\text{C}$  during 10000 seconds.

As it can be seen from Figs. 5 and 6 and Table 3, the initial creep strain or compliance have considerably decreased for all the specimen codes 3 to 5 which could be a sign of higher stiffness due to the presence of MGP, tending to maintain the specimen strain at a lower level. This could be an excellent method for designing pieces where large amounts of strain are not allowed. But the predicted failure time does not make any difference between the specimens with MGP and without MGP. The reason behind is that the effect of MGP is on the matrix not fiber and the fiber is ruling phase in creep test. Specifically, the matrix approaches to be ruined after some days. Though initial strain and initial strain rate during the first minute of the test performance for GFRE are less than those of BFRE at  $T=150\text{ }^{\circ}\text{C}$  and  $200\text{ }^{\circ}\text{C}$ , it is clearly observed from Figs. 5 and 6 that the slope of the GFRE compliance is much more than that of BFRE during the whole test and therefore, creep resistance of BFRE is superior to that of GFRE

#### 4. Conclusions

For the first time, micro glass powder was added into epoxy reinforced Unidirectional Basalt Fiber in order to investigate creep properties. In addition to it, creep properties of unidirectional glass fiber reinforced epoxy and unidirectional basalt fiber reinforced epoxy were compared to each other. Achieved results show that:

- 1- Using micro glass powder decreases the initial compliance as well as initial strain rate but does not have any noticeable effect on overall life time. Therefore, adding micro glass powder can be considered as a way for reducing initial strain and strain rate.
- 2- Basalt fiber is more creep resistant than glass fiber so it seems appropriate that basalt fiber be used instead of glass fiber for applications in which a high creep resistance is required.

3- BFREs and GFRE generally behave as non-linear for all stresses and temperatures under creep loads.

#### References

- [1] Valery, V.; Vasiliev, E.; Morozov, V., "Advanced Mechanics of Composite Materials", *Elsevier Publication*, First edition, 2007.
- [2] Kawai, M.; Sagawa, T., "Temperature dependence of off-axis tensile creep rupture behavior of a unidirectional carbon/epoxy laminate", *Composites: Part A*, 2009, 39, 523–539.
- [3] Dasappa, P.; Sullivan, P. L.; Xiao, X., "Temperature effects on creep behavior of continuous fiber GMT", *Composite: Part A*, 2009, 40, 1071-1081.
- [4] Kouadri-Boudjelthia, A.; Imad, A.; Bouabdallah, A.; Elmequenni, M., "Analysis of the effect of temperature on the creep parameters of composite material", *Materials and Design*, 2009, 30, 1569–1574.
- [5] Guedes, R. M.; Sa', A.; Faria, H., "Influence of moisture absorption on creep of GRP composite pipes", *Polymer Testing*, 2007, 26, 595–605.
- [6] Goertzen, W. K.; Kessler, M. R., "Creep behavior of carbon fiber/epoxy matrix composites", *Materials Science and Engineering A*", 2006, 421, 217–225
- [7] Feng, C. W.; Keong, C. W.; Hsueh, Y. P.; Wang, Y. Y.; Sue, H. J., "Modeling of long-term creep behavior of structural epoxy adhesives", *International Journal of Adhesion & Adhesive*, 2005, 25,427.
- [8] Khalili, S. M. R.; Jafarkarimi, M. H.; Abdollahi, M. A., "Creep analysis of fibre reinforced adhesives in single lap joints—Experimental study", *International Journal of Adhesion & Adhesive*, 2009, 29, 656-661.
- [9] Dean, G., "Modelling non-linear creep behaviour of an epoxy adhesive", *International Journal of Adhesion & Adhesive*, 2007, 27, 636-646.

- [10] Khalili, S. M. R.; Daghigh, V.; Eslami Farsani, R., "Mechanical behavior of basalt fiber-reinforced and basalt fiber metal laminate composites under tensile and bending loads", *Reinforced Plastics & Composites*, 2011, 30, 647-659.
- [11] Wei, Bin.; Song, Sh.; CaoMaterials, H., "Strengthening of basalt fibers with nano-SiO<sub>2</sub>-epoxy composite coating", *Materials & Design*, 2011, 32, 4180-4186.
- [12] Lopresto, V.; Leone, C.; De Iorio, I., "Mechanical characterisation of basalt fibre reinforced plastic", *Composite Part B: Engineering*, 2011, 42, 717-723.
- [13] Colombo C., Vergani L., Burman M., "Static and fatigue characterisation of new basalt fibre reinforced composites", *Composite Structure*, In Press. Available online 14 October 2011.
- [14] Wei Bin, Cao Hailin, Song Shenhua., "Environmental resistance and mechanical performance of basalt and glass fibers", *Materials Science and Engineering*, 2010, A 527, 4708-4715.
- [15] Wei Bin, Cao Hailin, Song Shenhua, "Tensile behavior contrast of basalt and glass fibers after chemical treatment", *Materials & Design*, 2010, 31, 4244-4250.
- [16] Carmisciano, S.; Igor, M. D. R.; Sarasini, F.; Tamburrano, A.; Valente, M., "Basalt woven fiber reinforced vinylester composites: Flexural and electrical properties", *Materials & Design*, 32, 337-342.
- [17] Wei, B.; Cao, H.; Song, Sh., "Degradation of basalt fibre and glass fibre/epoxy resin composites in seawater", *Corrosion Science*, 2011, 53, 426-431.
- [18] Fiore, V.; Di Bella, G.; Valenza, A., "Glass-basalt/epoxy hybrid composites for marine applications", *Materials & Design*, 2011, 32, 2091-2099.

Archive of SID